BIOCHEMISTRY
including biophysical chemistry & molecular biology

Article

pubs.acs.org/biochemistry

^{2}H Solid-State Nuclear Magnetic Resonance Investigation of Whole *Escherichia coli* Interacting with Antimicrobial Peptide MSI-78

James Pius,[†] Michael R. Morrow,[‡] and Valerie Booth*[,†,‡]

[†]Department of Biochemistry, Memorial University of Newfoundland, St. John's, NL, Canada A1B 3X9

[‡]Department of Physics and Physical Oceanography, Memorial University of Newfoundland, St. John's, NL, Canada A1B 3X7

ABSTRACT: A key aspect of the activity of antimicrobial peptides (AMPs) is their interaction with membranes. Efforts to elucidate their detailed mechanisms have focused on applying biophysical methods, including nuclear magnetic resonance (NMR), to AMPs in model lipid systems. However, these highly simplified systems fail to capture many of the features of the much more complex cell envelopes with which AMPs interact in vivo. To address this issue, we have designed a procedure to incorporate high levels of ^{2}H NMR labels specifically into the cell membrane of *Escherichia coli* and used this approach to study the interactions between the AMP MSI-78 and the membranes of intact bacteria. The ^{2}H NMR spectra of these membrane-deuterated bacteria can be reproduced in the absence and presence of MSI-78. Because the ^{2}H NMR data provide a quantitative measure of lipid disorder, they directly report on the lipid bilayer disruption central to the function of AMPs, in the context of intact bacteria. Addition of MSI-78 to the bacteria leads to decreases in the order of the lipid acyl chains. The molar peptide:lipid ratios required to observe the effects of MSI-78 on acyl chain order are approximately 30 times greater than the ratios needed to observe effects in model lipid systems and approximately 100 times less than the ratios required to observe inhibition of cell growth in biological assays. The observations thus suggest that MSI-78 disrupts the bilayer even at sublethal AMP levels and that a large fraction of the peptide does not actually reach the inner membrane.

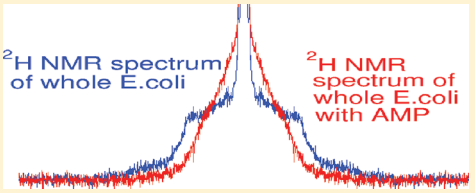

Demand for new antibiotics to combat the resistance of pathogens to conventional antibiotics[1] has led to heightened interest in the identification of peptides with antibacterial activity, termed antimicrobial peptides (AMPs).[2−4] Our natural defenses against pathogens rely heavily on the innate immune system, of which AMPs are an integral part.[5,6] In addition to their presence in humans, AMPs have also been identified in a variety of invertebrate, plant, and animal species and can display antimicrobial activity against bacteria, viruses, protozoa, and various other pathogens.[7,8] Structurally, they are frequently short cationic peptides, with a large subset of them being composed of amphipathic helices.

AMPs are generally thought to kill cells by disrupting their lipid bilayer membranes, although some likely interact with membranes only to gain access to targets inside the cell.[9−11] Some AMPs have also been shown to modulate innate immune responses and affect gene expression.[12−14] Because interactions of AMPs with lipid membranes are key in their mechanism of action, solid-state NMR spectroscopy has been a key method for studying these interactions at high resolution.[8,15,16] Such studies have reported the effect of the AMPs on overall bilayer structure, lipid acyl chain order, and headgroup tilt, while also providing information about the structure and positioning of the peptide in the bilayer.[17] Other important techniques for studying the mechanism of AMPs include molecular dynamics simulations, differential scanning calorimetry, dye release assays, ANS uptake assays, atomic force microscopy, and scanning electron microscope imaging.[18−21]

A crucial point with regard to the use of these techniques to study AMP mechanisms is that they have been predominantly applied to model lipid bilayers. In reality, there is a plethora of additional factors present in real microbial cell envelopes that likely affect how the peptides interact with the lipid bilayers. These include membrane proteins, the peptidoglycan layer, lipopolysaccharide, bilayer asymmetry,[22] and lipid domains.[23] One way to illustrate the enormous gap between the conditions under which the biological activity of AMPs is observed and the conditions under which solid-state NMR and other biophysical studies of mechanism are conducted is to consider the difference in peptide:lipid molar (P:L) ratios in the two circumstances. Solid-state NMR and other biophysical studies of model systems can typically show AMP-induced changes at peptide:lipid ratios close to 1:100. Strikingly, however, a ratio of 100 bacterially bound peptides per lipid is needed to see inhibition in an *Escherichia coli* sterilization assay, i.e., 10000 times more peptide per lipid.[24] At the other extreme, some workers have wondered how AMP concentrations high enough to have an impact are achieved in vivo and have attempted to provide an explanation based on the high membrane-bound concentrations of AMPs that can be achieved even at relatively low solution concentrations.[25]

While there is a body of work substantiating the "self-promoted uptake" mechanism by which AMPs may traverse the outer membrane of bacteria (e.g., ref 26) and a handful of solid-state NMR studies of AMPs have been performed with bacterial

Received: October 11, 2011
Revised: November 28, 2011
Published: November 29, 2011

lipid extracts (e.g., ref 27), to the best of our knowledge there is no published work that applies high-resolution techniques such as NMR to the study of AMPs in intact bacteria.

To bridge the gap between the NMR studies of AMPs that employ model membranes and the functional mechanism in intact cells, we have developed an approach to apply ^{2}H NMR to intact bacteria treated with AMPs. Because mutated strains of *E. coli* used for ^{2}H NMR in the past[28] are no longer available, this involved creating a new strain of *E. coli*, termed LA8, that allows us to incorporate high levels of isotope labels, in this case ^{2}H, specifically into the acyl chains of lipid membranes. This was done by modifying *E. coli* strain L8, which already has a mutation that affects total fatty acid synthesis (*fabE*),[29] to be also deficient in fatty acid metabolism, via a mutation in *fadE*. The combined effects of these modifications allow for the incorporation of labeled fatty acids specifically into the membrane by supplementing the growth medium with them.

For this study, we chose to treat the ^{2}H membrane-labeled *E. coli* with a well-studied, highly active AMP. MSI-78 is a synthetic peptide analogue of magainin 2, which is found in the skin of bullfrogs.[30] It is a very potent hydrophilic antibiotic with an MIC value of 4 μg/cell, a net cationic charge of +9, and a grand average hydropathicity index of −0.159.[31] MSI-78 is unstructured in aqueous medium but adopts a helical conformation when it interacts with membranes.[32] NMR studies indicate it tends to be oriented nearly perpendicularly with respect to the bilayer normal, inducing a positive curvature strain on lipid bilayers consistent with formation of torroidal pores, which may lead to cell death.[31]

MATERIALS AND METHODS

Peptide Preparation. MSI-78 (NH_2-GIGKFLKKAKKFG-KAFVKILKK-NH_2) was synthesized via solid phase methods employing *O*-fluorenylmethyl-oxycarbonyl (Fmoc) chemistry and purified using HPLC with a preparative scale reverse phase C8 column, as described in ref 33. Mass spectroscopy was used to select the HPLC fractions with high-purity MSI-78. Stock solutions of MSI-78 were prepared by dissolving the peptide in Medium 63.[34]

Preparation of LA8 Bacteria. Starting with the L8 strain of bacteria obtained from the Coli Genetic Stock Center (CGSC, Yale University, New Haven, CT), we introduced genetic manipulations to replace the *fadE* gene (needed for fatty acid metabolism) with a kanomycin resistance gene, using the method of Datsenko and Wanner.[35] The L8 strain was transformed with plasmid pKD46 encoding the λ Red recombinase system and then grown in 2 mL of minimal growth medium with ampicillin (50 μg/mL) and L-arabinose (10 mM) at 30 °C to an A_{600} of ≈0.6. Then the cells were made electrocompetent by being washed twice with ice-cold 10% glycerol and concentrated 20-fold. PCR was used to construct a linear piece of DNA containing the kanamycin resistance gene (*kan*), flanked by sequences homologous to the start and stop regions of the *fadE* gene. Two primers, along with pKD4, a template plasmid carrying the *kan* gene between the P1 and P2 sites, were used to synthesize the linear *kan* gene. The forward primer has a sequence that is homologous to that of the start codon of the *fadE* gene at the 5′ end and a sequence that is homologous to that of the P1 site of pKD4 at the 3′ end.[36] The reverse primer has a sequence that is homologous to that of the reverse complement of the stop codon region of the *fadE* gene at its 5′ end and a sequence that is homologous to that of the P2 site of pKD4 at the 3′ end.[36] PCR was conducted using *Pfu* DNA polymerase (Stratagene), according to the manufacturer's instructions. The purified PCR product was electroporated into the transformed electrocompetent L8 cells using a cell porator. One milliliter of medium was added to the shocked cells, and they were quickly transferred to a sterile culture tube and incubated at 37 °C for 2 h with moderate shaking. Aliquots of the culture were then plated on selective medium containing 30 μg/mL kanamycin. Kanamycin-resistant colonies were isolated and cultured in liquid medium and stored at −80 °C in 50% glycerol until they were needed. The presence of the *kan* gene in the proper orientation in these mutants (LA8) was confirmed via PCR.

The minimal growth medium used for all strains was Medium 63[34] supplemented with 0.4% glycerol, 1 μg/mL thiamine, 0.3% casamino acids, and 0.1% Brij-58. This supplemented medium is termed Medium 63-A. Another medium used in the study was Medium 63-A supplemented with 50 μg/mL deuterated palmitic acid and 50 μg/mL oleic acid and is termed Medium 63-B. Deuterated (d_{31}) palmitic acid and unlabeled oleic acid were purchased from Sigma-Aldrich (St. Louis, MO). Additionally, for the LA8 strain, the medium was inoculated with 30 μg of kanamycin/mL of medium. Strain LA8 was grown at 30 °C in Medium 63-A (without fatty acid supplements) overnight and subcultured at 37 °C in fresh Medium 63-B (supplemented with fatty acids). Solid medium plates were prepared using the liquid Medium 63-B with 1.5% agar.

Plate-Count Assay. Pre- and post-NMR bacterial samples were diluted in series using Medium 63; 50 μL of the diluent was then spread onto a solid medium plate. The plates where incubated overnight at 37 °C. Only those plates that contained between 30 and 300 well-separated colonies were used in determining the number of cells in the original sample.

Preparation of Treated and Untreated Cells for NMR. LA8 bacteria were harvested in midlog phase at an A_{600} of 0.6−1.0. The cells were centrifuged at 4 °C for 10 min at 4100*g*. For studies of untreated cells, the bacteria were then washed with gentle agitation for 15 min in 100 mL of Medium 63 (with no supplements) containing 0.1% Brij-58. The sample was centrifuged as before, and the pellet was then used immediately for ^{2}H NMR studies. For bacteria treated with peptide, additional steps were taken; after the washing and centrifugation step described above, the pellet was resuspended by gentle agitation in 100 mL of Medium 63 for 15 min. Then the appropriate amount of peptide was added and subjected to mild shaking for 5 min. This sample was centrifuged as described above and used for NMR. Samples were transferred into the NMR sample holder using a sterile spatula. Control experiments with buffer (Medium 63) in place of AMP demonstrated that the additional 15 min resuspension and treatment steps employed for the AMP-treated bacteria led to decreases in M_1 of less than 2.3%.

The peptide concentration for each sample indicated in the figures was expressed as the weight percentage (peptide weight/dry cell weight). To measure the dry weight of bacteria, we grew samples at absorbances (A_{600}) between 0.6 and 1.0 and processed them in a manner similar to that described above. The resulting pellet was then dried under vacuum for 48 h and weighed on an analytical balance. The data were used to create a standard curve (data not shown) relating the absorbance to the measured dry weight of bacteria, which was used to determine dry cell weight in samples containing peptide.

NMR Experiments. ^{2}H NMR experiments were performed at 37 °C on an in-house-assembled 9.4 T solid-state NMR spectrometer operated at a resonance frequency of 61.42 MHz for ^{2}H nuclei. A quadrupole echo pulse sequence ($\pi/2$−t−$\pi/2$−acq) was used as described elsewhere,[37] using a 900 ms recycling delay, a 30 μs pulse separation, and a 5 μs pulse duration. Data were collected using a 1 μs dwell time and 8192 points. Oversampling by a factor of 4 was applied to give an effective dwell time of 4 μs. The free induction decay was shifted to the left to place the echo maximum at the first point. Transients were averaged in sequential blocks of 8000 scans, each collected over 2 h, to allow for monitoring of time-dependent changes in the spectral shape. For the comparison of samples containing different peptide concentrations, 32000 transients were averaged for each spectrum displayed. For calculations of moments, the imaginary channel was set to zero before Fourier transformation to symmetrize the spectra.

Echo decay times, T_{2e}, were measured for each sample by varying the quadrupole echo sequence pulse separation, τ, sequentially from 30 to 400 μs. For each pulse separation, 2000 transients were averaged to obtain the echo amplitude. The mean echo decay rates, $\langle 1/T_{2e}\rangle$, were obtained from fits to the initial echo decay according to

$$A_0(2\tau) = A_0(0)\mathrm{e}^{-2\tau\langle 1/T_{2e}\rangle} \quad (1)$$

where A_0 is the maximal amplitude of the echo. The reported echo decay times are the inverse of the mean echo decay rate.[38]

Moment Analysis. First spectral moments, M_1, were calculated from the symmetric ^{2}H NMR powder pattern spectra according to

$$M_1 = \frac{\int_0^\infty \omega f(\omega)\, \mathrm{d}\omega}{\int_0^\infty f(\omega)\, \mathrm{d}\omega} \quad (2)$$

where ω is the frequency with respect to the central Larmor angular frequency ω_o and $f(\omega)$ is the line shape.[28] The first moment is proportional to the average quadrupole splitting in the spectrum and thus to the average of the deuteron orientational order parameter

$$S_{CD} = \frac{1}{2}\langle 3\cos^2\theta - 1\rangle \quad (3)$$

over the deuterated chains. In eq 3, θ is the angle between the C−D bond, on a given chain segment, and the bilayer normal that is the axis about which the chain undergoes fast, axially symmetric reorientation.[39]

Second spectral moments, M_2, were also calculated from the symmetric powder patterns according to

$$M_2 = \frac{\int_0^\infty \omega^2 f(\omega)\, \mathrm{d}\omega}{\int_0^\infty f(\omega)\, \mathrm{d}\omega} \quad (4)$$

Second moments were used to calculate the parameter

$$\Delta_2 = \frac{M_2}{1.35 \times {M_1}^2} - 1 \quad (5)$$

which is the relative mean square width of the distribution of orientational order parameters[28] and is thus sensitive to the shape of the spectrum.

For each spectrum, baselines for the integrals in eqs 2 and 4 were obtained by averaging all points in the range of 33.6−45.8 kHz. For samples with no peptide, integrals ran from 0 to 29.3 kHz. For peptide-containing samples, the intensity reaches the baseline at lower frequencies and the integrals were cut off at 24.4 kHz. For all spectra, the narrow feature at the spectral center, corresponding to isotropically reorienting natural abundance deuterated water, was clipped between ±0.4 kHz by setting the intensity in that range to the average of the intensity in the range of 0.4−0.5 kHz. The spectrometer control and analysis software was developed in house and modeled closely on programs originally developed by Davis and co-workers.[39]

RESULTS

For ^{2}H NMR studies of entire bacteria, it was desirable to maximize the level of ^{2}H labeling in the lipid membranes and minimize the ^{2}H background signal from elsewhere in the bacteria. To accomplish this, we prepared a strain of *E. coli*, termed LA8, that is unable to synthesize or metabolize fatty acids, allowing for selective ^{2}H labeling of the saturated chains of most phospholipids via incorporation of ^{2}H-labeled palmitic acid into the growth medium.[28] The starting point for producing LA8 was the L8 strain of bacteria, which has a mutation that makes it unable to synthesize fatty acids.[29] Using the system of Datsenko and Wanner,[35] as described in detail in Materials and Methods, genetic manipulations were introduced to also remove the ability of these bacteria to metabolize fatty acids, by replacing the *fadE* gene with a kanamycin resistance gene, *kan*. On the basis of the similarity between the LA8 and L51 strains,[28] along with the growth protocol employed, we expect 96% of the phosphatidylethanolamine (PE), the major phospholipid in the bacterial membrane,[40] to have a deuterated palmitic acid at the *sn*-1 position.

Growth curves were measured for the LA8 bacteria (Figure 1), and it was found that the midlog phase of growth occurs 6−7 h after inoculation of the overnight culture into fresh medium. ^{2}H NMR spectra were recorded for cells harvested during the midlog phase, during the stationary phase, and during the early log phase (data not shown). These confirmed that cells from the midlog phase gave the best spectra; cells harvested in the later phases gave rise to spectra with poor signal-to-noise ratios, presumably as a result of the physiological effects associated with reduced levels of nutrients.

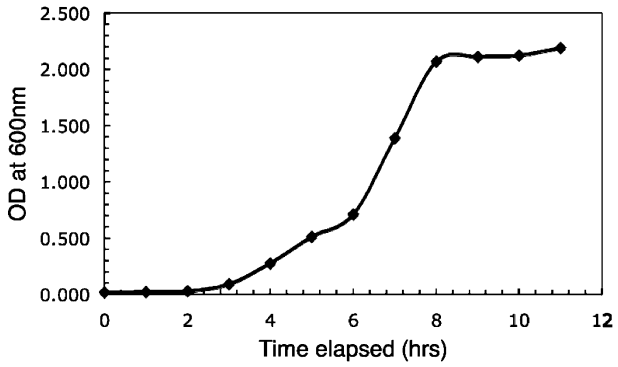

Figure 1. Growth of LA8 bacteria as measured by absorbance at 600 nm, |OD_{600}|. Cells were inoculated from an overnight culture at time zero and then grown at 37 °C in minimal medium supplemented with oleic acid and palmitic acid.

The next tasks were to assess the stability and reproducibility of the ^{2}H NMR spectra acquired for the ^{2}H membrane-labeled

dx.doi.org/10.1021/bi201569t | *Biochemistry* 2012, 51, 118−125

LA8 bacteria. Figure 2a shows a series of spectra acquired at 37 °C every 2 h, such that the first scan starts 2 h after the initial

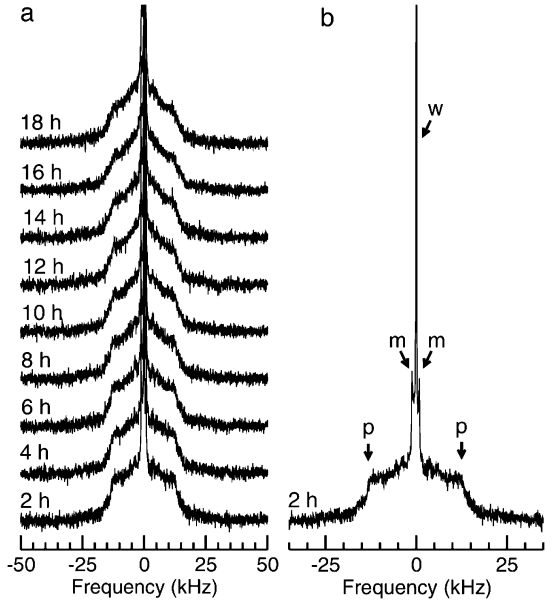

Figure 2. (a) Solid-state ^{2}H NMR spectra of membrane-deuterated LA8 bacteria, showing the evolution of the NMR spectra over time. Experiments were performed at 37 °C, and each spectrum represents 8000 scans. (b) Isolated trace of the 2 h spectrum with arrows to indicate the water peak (w), palmitate methyl deuteron doublet (m), and prominent edges (p) corresponding to the quadrupole splitting deuterons near the headgroup, and thus most motionally constrained, end of the acyl chain. This feature is typically associated with the plateau region of the orientational order parameter profile.

harvesting of the log phase bacteria. Figure 2b isolates the spectrum at 2 h and illustrates some of the spectral features. These spectra at 37 °C display a prominent shoulder near ±12 kHz and thus resemble spectra from lipid liposomes just above their gel to liquid crystalline transition temperature (e.g., refs 28 and 41). The shoulder at approximately ±12 kHz, indicated by arrows labeled p in Figure 2b, arises from deuterons on the motionally constrained region of the deuterated palmitate chains near the headgroup and corresponds to the plateau region of the orientational order parameter profile.[39,42] The quadrupole splittings decrease with the proximity of the deuterated chain segment to the bilayer center. The doublet arising from methyl groups at the deuterated chain ends is labeled with an m in Figure 2b. All of the spectra also have a sharp, central peak with a width of <1 kHz, which arises from naturally occurring deuterated water.[28] This feature is labeled with a w in Figure 2b. As time progresses, there is a decrease in the intensity at the larger splittings and an increase in the intensity at the lower splittings, indicating an increase in the lipid acyl chain disorder over time.

To quantify the changes in the spectra that occur with time, we calculated the first moments, M_1, that are proportional to the average order parameter of the ^{2}H-labeled lipid acyl chains. We also calculated the second moment, M_2, and the mean square width of the distribution of splittings, Δ_2. As one can see in the top curve in Figure 3a, the first moment M_1 decreases slowly with time, reflecting an overall decrease in the average order parameter because of the increased amplitude of motions of the acyl chains in the bacterial membrane. Over the course of

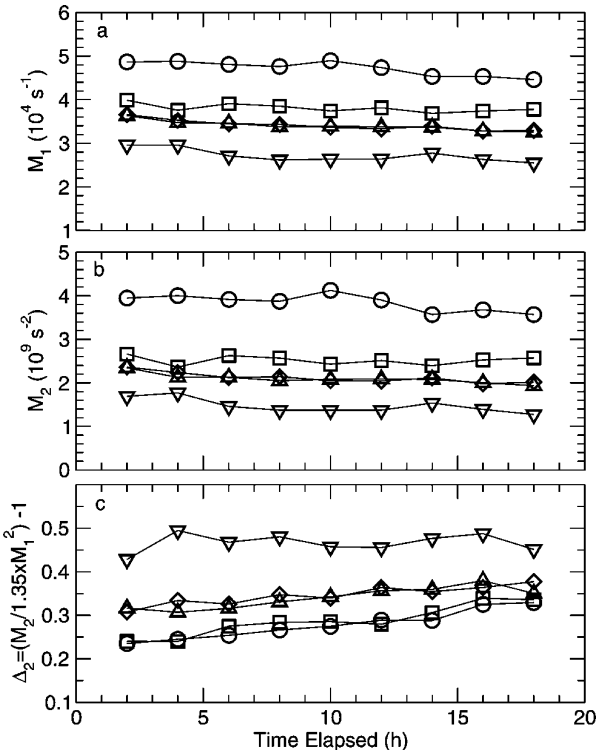

Figure 3. (a) First moment M_1, (b) second moment M_2, and (c) Δ_2 of ^{2}H NMR spectra from membrane-deuterated LA8 bacteria as a function of time in the presence of increasing concentrations of MSI-78. Time zero refers to the moment the NMR study began following sample processing, i.e., 2 h after the cells were initially harvested. Concentrations of MSI-78 (w/w) were (○) 0% peptide, (□) 10% peptide, (◇) 20% peptide, (△) 30% peptide, and (▽) 60% peptide.

18 h, M_1 values for the untreated bacteria decrease from an initial value of ~5 × 10^4 s^{-1} to a value of ~4.5 × 10^4 s^{-1}. The bacterial membranes are only slightly less ordered than model lipid membranes such as those of multilamellar vesicles composed of DPPC-d_{62}, which typically exhibit M_1 values of ~5 × 10^4 s^{-1} just above their transition temperature.[43,44]

Figure 3b shows corresponding values of the second spectral moment, M_2. Because of the differences in how intensity at a given splitting contributes to the first and second moments, an appropriate comparison of these moments can be sensitive to spectral shape. This comparison is provided by the equation $\Delta_2 = (M_2/1.35 \times M_1^2) - 1$, the relative mean square width of the distribution of orientational order parameter. In Figure 3c, Δ_2 increases as the spectral shape changes from having more prominent shoulders near ±12 kHz to having less prominent shoulders and relatively more intensity at smaller splittings.

In preparing the bacteria for NMR, we washed the cells and resuspended them in buffer (Medium 63). Thus, the change in spectral shape reflected by the slow reduction in M_1, and corresponding changes in M_2 and Δ_2, over time is likely related to the absence of nutrients available to the cells while they are in the NMR spectrometer. Cell viability assays were therefore conducted under conditions identical to those used in the NMR experiments (Figure 4). The initial washing of the bacteria leads to a loss of 45% of the viable cells on average. Six hours after being washed, i.e., after the first three spectra shown in Figure 2a, on average, 76% of these cells are still capable of forming colonies. After 12 and 18 h, approximately 50% of the cells that went into the NMR spectrometer retained their ability

dx.doi.org/10.1021/bi201569t | *Biochemistry* 2012, 51, 118−125

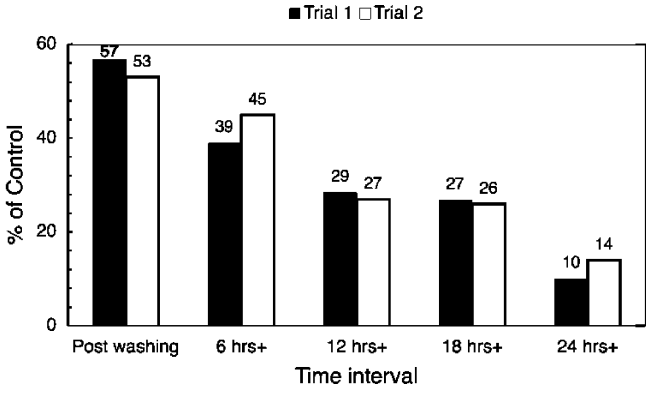

Figure 4. Plate counts for cells plated immediately after processing and before the NMR experiments, as well as for cells held under conditions identical to those for NMR studies and plated after 6, 12, 18, and 24 h. The percentages are relative to those of unprocessed cells plated before washing. Two separate experiments were performed at each time point.

to form colonies. The rate of loss of colony forming ability was thus quite high compared to the rate of decrease in M_1. This suggests that cell death may not be accompanied by large changes in M_1 and/or that a substantial population of bacteria do not necessarily die during the NMR experiment but do lose their ability to form colonies within the time span of this assay.

Figure 5a shows ^{2}H NMR spectra of ^{2}H membrane-labeled LA8 bacteria treated with varying concentrations of the antimicrobial peptide MSI-78. These spectra represent averages of the first 8 h of data collection and thus show better signal:noise ratios compared to the spectra displayed in Figure 2a, which represent 2 h scans. Treatment with MSI-78 resulted in growth of the intensity at smaller splittings relative to that at larger splittings, indicating a decrease in average orientational order with increasing amounts of MSI-78 used in the treatment. Significantly, the quadrupole splitting corresponding to the spectral shoulder (arrows in Figure 5a) is found to decrease with an increasing peptide concentration. The spectra may still reflect a shift in the relative populations of more and less ordered membrane regions, but in contrast to the changes with time shown in Figure 2a, there is no fraction of the membrane for which orientational order is not diminished as peptide concentration increases. Panels b–d of Figure 5 show the dependence of M_1, M_2, and Δ_2, respectively, on peptide concentration for the spectra in Figure 5a and those for two duplicate samples prepared with no peptide and 30% (w/w) MSI-78. These panels clearly show the effect of the peptide on both the average orientational order along the deuterated chain (M_1) and the distribution of intensity across the spectrum (Δ_2).

As with the untreated cells, the shape of the spectra for the MSI-78-treated bacteria was quantified in terms of M_1, M_2, and Δ_2, calculated for each 2 h of NMR data acquisition, and plotted in panels a–c of Figure 3, respectively. For the treated bacteria, the slow changes in M_1, M_2, and Δ_2 over time occurred at roughly the same rate as in the untreated bacteria. However, each M_1, M_2, or Δ_2 versus time curve was displaced, in response to MSI-78 treatment, to an extent consistent with the peptide concentration dependencies illustrated in panels b–d of Figure 5, respectively. In general, increasing concentrations of MSI-78 resulted in lower values of M_1 and M_2, although the values for 20 and 30% peptide (w/w, peptide wight/dry cell weight) were similar. The response of Δ_2 to peptide concentration is opposite that of M_1 and M_2, reflecting its sensitivity to spectral shape rather than simply width. The reductions in M_1 with peptide treatment are substantial. For example, with 20% MSI-78, the initial M_1 is ~20% lower than

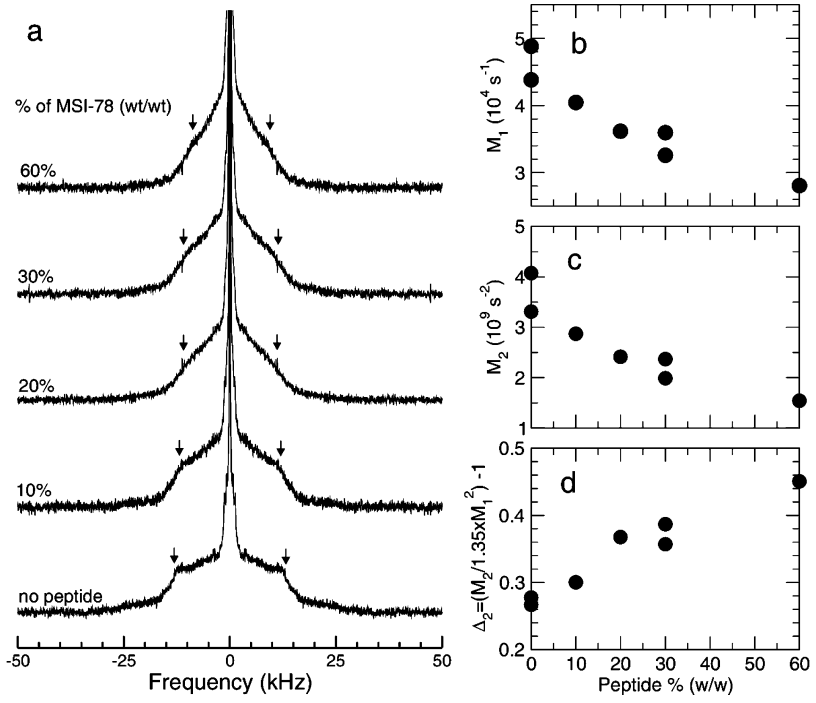

Figure 5. (a) Solid-state ^{2}H NMR spectra of membrane-deuterated LA8 bacteria with increasing concentrations of MSI-78. MSI-78 concentrations are quoted as the weight of MSI-78 per dry weight of bacteria × 100. NMR experiments were performed at 37 °C, and each spectrum represents 32000 scans. The right panel shows (b) first moment M_1, (c) second moment M_2, and (d) Δ_2 vs peptide concentration for the spectra in panel a and the spectra of duplicate samples at peptide concentrations of 0 and 30%.

dx.doi.org/10.1021/bi201569t | *Biochemistry* 2012, 51, 118–125

that for the untreated cells. The decrease in the initial M_1 with an increasing peptide concentration is also large when compared to the change in M_1, observed for all the samples over the total experiment time of 18 h. The results displayed in panels b–d of Figure 5 for duplicate untreated and 30% peptide samples illustrate reproducibility, particularly for Δ_2, which, because it depends on the ratio of M_2 to M_1^2, is less sensitive to baseline imperfection.

The effects of MSI-78 on bacterial membranes were also investigated by measuring the quadrupolar echo decay time, T_{2e}, of LA8 with varying peptide concentrations (Figure 6).

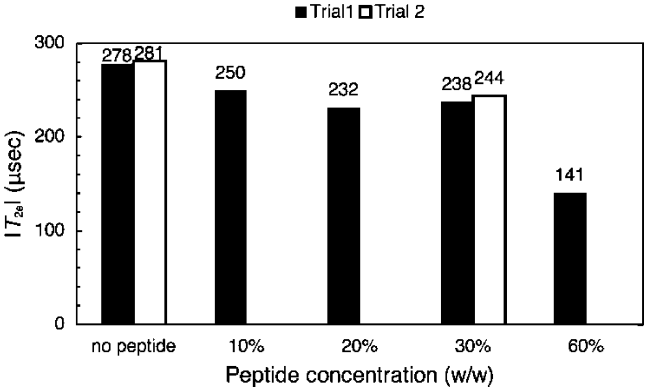

Figure 6. NMR quadrupolar echo decay time, $|T_{2e}|$, at 37 °C for membrane-deuterated LA8 bacteria, showing the effect of increasing concentrations of MSI-78.

Quadrupole echo decay reflects motions that change the orientation-dependent quadrupole interaction on a time scale comparable to the time over which the echo is formed. In the liquid crystalline phase, quadrupole echo decay can reflect slow motions, like bilayer undulations, and faster motions, like lipid wobble and reorientation about the bilayer normal, that both contribute to narrowing of the observed spectrum.[45] For such faster motions, the contribution to the echo decay rate is proportional to the second moment of that portion of the quadrupole moment modulated by the motion, a parameter related to the amplitude of the motion, and the correlation time for that motion. It is interesting that the quadrupole echo decay times observed here, and summarized in Figure 6, are somewhat low compared to those normally seen in the liquid crystalline phase of model bilayers.[46] This may reflect a larger range of lipid chain reorientation in the more compositionally heterogeneous environment of the natural membrane.

For most of the peptide concentrations used, the effect on T_{2e} is quite modest. However, for 60% MSI-78 (w/w), there is a substantial drop in T_{2e}, perhaps indicating that the bilayers are starting to lose integrity on a larger scale and that the average angular range of lipid reorientation is increasing, as suggested by the observed decrease in the average quadrupole splitting.

DISCUSSION

This study provides, to the best of our knowledge, the first NMR observation of AMP-induced lipid membrane disruption in whole bacteria. Substantial and reproducible changes in the overall orientational order, M_1, the second moment, M_2, and the relative mean square width of the splitting distribution, Δ_2, derived from spectra of ^{2}H membrane-labeled *E. coli* were observed upon addition of the AMP MSI-78 (Figures 3 and 5). Decreases in the orientational order parameter derive from increases in lipid disorder (increased angular amplitude of lipid chain motions), and thus, M_1 directly reports on the lipid bilayer disruption proposed to be central to the function of AMPs. Changes in M_2 and Δ_2 provide additional characterization of how the spectral shape changes in response to peptide-induced disruption. A key consideration with regard to the utility of ^{2}H measuments in whole bacteria is that solid-state NMR studies of AMPs in model lipid bilayers have been one of the cornerstones of the study of AMP mechanisms. Thus, comparing the results of NMR data in whole bacteria and model lipid system should provide useful insights into the interpretation of AMP effects in vivo.

For such comparisons to be meaningful, it was important to first characterize the ^{2}H membrane-labeled bacteria employed in the NMR studies. To achieve high and specific levels of incorporation of the ^{2}H label, we produced a novel strain of *E. coli* deficient in both fatty acid synthesis and catabolism, termed LA8. The LA8 bacteria were similar to the L51 strain used in studies of bacterial membranes in the 1970s,[28] and our untreated bacteria gave rise to similar NMR spectra at 37 °C. The stability of the ^{2}H NMR spectra of the ^{2}H membrane-labeled LA8 cells was characterized over time. A slow change in spectral moments was observed over the 18 h experiment, which is not surprising, as the cells do not have access to nutrients during the NMR experiment. The spectral change over this period was small compared to the effect of treatment with peptide, and the rate of change was similar for all samples assayed, both treated and untreated. Likewise, duplicate experiments with fresh bacterial cell preparations confirmed these observations for both control and AMP-treated cells. Thus, it appears that the effects of the AMP treatments are present before the NMR experiments begin. The absence of any AMP-induced change in the M_1 versus time slope is consistent with the low levels of AMP used relative to the MIC and allows us to compare the effect of the peptide on the spectra using an average of the first 8 h of NMR data acquired.

To compare the NMR data from the ^{2}H membrane-labeled cells to NMR data from model lipid systems or to cell growth AMP inhibition assays, it is useful to recalculate the amounts of AMP used in terms of molar peptide:lipid (P:L) ratios, in particular in terms of bacterium-bound P:L ratios. Typically, 10–95% of an AMP binds to the bacteria within 10–15 min.[24,47] Because MSI-78 has an overall charge of +9, it would be expected to bind more tightly and quickly than an average AMP and so is likely to be closer to the top of this 10–95% range. When calculated assuming 100% of MSI-78 is bacterial-bound, the w/w peptide:bacterium ratios used in this study of 10, 20, 30, and 60% convert to molar bound P:L ratios of 0.31:1, 0.63:1, 0.94:1, and 1.9:1, respectively. This calculation uses our measurements of bacterial dry weight and assumes lipids comprise 9.1% of the bacterial dry weight and have an average molecular weight of 705 g/mol.[48]

Typical bound P:L ratios needed to inhibit bacterial growth in assays for AMP antimicrobial activity are 100:1.[24] This is ~100 times more peptide than the amount used in this study. It thus appears that the AMP–lipid interaction being observed in this work is in the sublethal range. Hence, we can conclude that some level of AMP-induced bilayer disruption does occur at levels well below those where cell growth inhibition takes place. This suggests some interesting possibilities regarding the two proposed classes of killing mechanisms for AMPs in general. For AMPs that are thought to act primarily by membrane disruption, it raises the possibility that a great deal of AMP-

induced membrane disruption can be tolerated before actual growth inhibition or cell death occurs. For AMPs that are thought to act on intracellular targets and whose interaction with the membrane is thus thought to be only that required to enter the cell, it suggests that even at relatively low levels of AMP, there is some bilayer disruption and a consequent increased permeability to the AMP.

On the other hand, the P:L ratio required to see reductions in lipid chain order in the ^{2}H membrane-labeled bacteria was much higher than those needed to see comparable changes in model lipid bilayers. Typical AMP:lipid ratios needed to see leakage in vesicle studies are 1:100 (total peptide) to 1:200 (bound peptide).[24] In ^{2}H NMR studies with model lipid membranes, AMP-induced decreases in lipid order are typically seen at ratios 1−3:100 or lower (e.g., refs 45 and 46). For MSI-78, Ramamoorthy et al.[31] showed dye leakage at P:L ratios as low 1:1000 (in POPC/POPG membranes) and observed a decrease in order parameter of ∼23% at a P:L ratio of 3:100. In the context of whole bacteria, the ratio of peptide required to produce comparable changes in chain order is ∼1:1 (Figures 3 and 5), i.e., ∼33 times higher than that used by Ramamoorthy et al.

There are at least two possible reasons why more peptide is needed to see comparable effects on the membrane of whole bacteria compared to model lipid bilayers. One possibility is that most of the peptide reaches the inner membrane but, for some reason, is less able to disrupt bilayer chain order at low concentrations than is the case in model systems where low concentrations are sufficient to cause observable effects. A more likely possibility, though, is that much of the peptide does not reach the inner membrane. It may be bound up in other components of the Gram-negative cell envelope, such as the LPS layer. Substantial and disruptive interactions between LPS and MSI-78's parent peptide, magainin 2, have previously been observed.[31,49,50] More generally, the importance of non-phospholipid components of the bacterial cell wall has been suggested, for example, by the existence of some AMPs that appear to be able to act without crossing the outer membrane of Gram-negative bacteria (e.g., ref 51) and on the basis of observations that cell wall thickness correlates with AMP resistance in methicillin-resistant *Staphylococcus aureus*.[52]

In conclusion, we have shown it is possible to obtain reproducible ^{2}H NMR spectra of membrane-deuterated LA8 bacteria in the absence and presence of the AMP MSI-78. The addition of MSI-78 leads to decreases in the order of the acyl chains in these bacteria. The P:L ratios needed to observe the effects of MSI-78 on acyl chain order is intermediate between the ratios required to observe effects in biophysical studies of model lipid systems and the ratios required to observe inhibition of cell growth in biological assays.

Abbreviations

AMP, antimicrobial peptide; ANS, 8-anilinonaphthalene-1-sulfonic acid; DPPC, dipalmitoylphosphatidylcholine; Fmoc, *O*-fluorenylmethyl-oxycarbonyl; HPLC, high-performance liquid chromatography; kan, kanamycin; LPS, lipopolysaccharide; M_1, first moment; NMR, nuclear magnetic resonance; P:L, peptide:lipid; PCR, polymerase chain reaction; POPC, 1-palmitoyl-2-oleoyl-*sn*-glycero-3-phosphocholine; POPG, 1-palmitoyl-2-oleoyl-*sn*-glycero-3-phosphoglycerol; *Pfu*, *Pyrococcus furiosus*; T_{2e}, echo decay time.

AUTHOR INFORMATION

Corresponding Author

*Department of Biochemistry, Memorial University of Newfoundland, St. John's, NL, Canada A1B 3X9. E-mail: vbooth@mun.ca. Phone: (709) 864-4523.

Funding

This research was supported by National Sciences and Engineering Research Council grants to V.B. and M.R.M. and a Master's research award to J.P. by the Research & Development Corp.

REFERENCES

(1) Boucher, H. W., Talbot, G. H., Bradley, J. S., Edwards, J. E., Gilbert, D., Rice, L. B., Scheld, M., Spellberg, B., and Bartlett, J. (2009) Bad bugs, no drugs: No ESKAPE! An update from the Infectious Diseases Society of America. *Clin. Infect. Dis. 48*, 1−12.

(2) Zasloff, M. (2002) Antimicrobial peptides of multicellular organisms. *Nature 415*, 389−395.

(3) Splith, K., and Neundorf, I. (2011) Antimicrobial peptides with cell-penetrating peptide properties and vice versa. *Eur. Biophys. J. 40*, 387−397.

(4) Rotem, S., and Mor, A. (2009) Antimicrobial peptide mimics for improved therapeutic properties. *Biochim. Biophys. Acta 1788*, 1582−1592.

(5) Yeung, A. T., Gellatly, S. L., and Hancock, R. E. (2011) Multifunctional cationic host defence peptides and their clinical applications. *Cell. Mol. Life Sci. 68*, 2161−2176.

(6) Patrzykat, A., and Douglas, S. E. (2005) Antimicrobial Peptides: Cooperative Approaches to Protection. *Protein Pept. Lett. 12*, 19−25.

(7) Brogden, K. A. (2005) Antimicrobial peptides: Pore formers or metabolic inhibitors in bacteria? *Nat. Rev. Microbiol. 3*, 238−250.

(8) Fernandez, D. I., Gehman, J. D., and Separovic, F. (2009) Membrane interactions of antimicrobial peptides from Australian frogs. *Biochim. Biophys. Acta 1788*, 1630−1638.

(9) Jenssen, H., Hamill, P., and Hancock, R. E. (2006) Peptide antimicrobial agents. *Clin. Microbiol. Rev. 19*, 491−511.

(10) Hale, J. D., and Hancock, R. E. (2007) Alternative mechanisms of action of cationic antimicrobial peptides on bacteria. *Expert Rev. Anti-Infect. Ther. 5*, 951−959.

(11) Cudic, M., and Otvos, L. J. (2002) Intracellular targets of antibacterial peptides. *Curr. Drug Targets 3*, 101−106.

(12) Bowdish, D. M., Davidson, D. J., and Hancock, R. E. (2005) A re-evaluation of the role of host defence peptides in mammalian immunity. *Curr. Protein Pept. Sci. 6*, 35−51.

(13) Tecle, T., Tripathi, S., and Hartshorn, K. L. (2010) Review: Defensins and cathelicidins in lung immunity. *Innate Immun. 16*, 151−159.

(14) Allaker, R. P. (2008) Host defence peptides: A bridge between the innate and adaptive immune responses. *Trans. R. Soc. Trop. Med. Hyg. 102*, 3−4.

(15) Bechinger, B. (2011) Insights into the mechanisms of action of host defence peptides from biophysical and structural investigations. *J. Pept. Sci. 17*, 306−314.

(16) Bhattacharjya, S., and Ramamoorthy, A. (2009) Multifunctional host defense peptides: Functional and mechanistic insights from NMR structures of potent antimicrobial peptides. *FEBS J. 276*, 6465−6473.

(17) Aisenbrey, C., Bertani, P., and Bechinger, B. (2010) Solid-state NMR investigations of membrane-associated antimicrobial peptides. *Methods Mol. Biol. 618*, 209−233.

(18) Marrink, S. J., de Vries, A. H., and Tieleman, D. P. (2009) Lipids on the move: Simulations of membrane pores, domains, stalks and curves. *Biochim. Biophys. Acta 1788*, 149−168.

(19) Joanne, P., Galanth, C., Goasdoue, N., Nicolas, P., Sagan, S., Lavielle, S., Chassaing, G., El Amri, C., and Alves, I. D. (2009) Lipid reorganization induced by membrane-active peptides probed using differential scanning calorimetry. *Biochim. Biophys. Acta 1788*, 1772−1781.

(20) Xiong, Y. Q., Mukhopadhyay, K., Yeaman, M. R., Adler-Moore, J., and Bayer, A. S. (2005) Functional interrelationships between cell membrane and cell wall in antimicrobial peptide-mediated killing of *Staphylococcus aureus*. *Antimicrob. Agents Chemother. 49*, 3114−3121.
(21) Shaw, J. E., Epand, R. F., Hsu, J. C. Y., Mo, G. C. H., Epand, R. M., and Yip, C. M. (2008) Cationic peptide-induced remodelling of model membranes: Direct visualization by in situ atomic force microscopy. *J. Struct. Biol. 162*, 121−138.
(22) Ruiz, N., Kahne, D., and Silhavy, T. J. (2006) Advances in understanding bacterial outer-membrane biogenesis. *Nat. Rev. Microbiol. 4*, 57−66.
(23) Epand, R. M., and Epand, R. F. (2009) Lipid domains in bacterial membranes and the action of antimicrobial agents. *Biochim. Biophys. Acta 1788*, 289−294.
(24) Wimley, W. C. (2010) Describing the mechanism of antimicrobial peptide action with the interfacial activity model. *ACS Chem. Biol. 5*, 905−917.
(25) Melo, M. N., Ferre, R., and Castanho, M. A. R. B. (2009) Antimicrobial peptides: Linking partition, activity and high membrane-bound concentrations. *Nat. Rev. Microbiol. 7*, 245−250.
(26) Piers, K. L., and Hancock, R. E. W. (1994) The interaction of a recombinant cecropin/melittin hybrid peptide with the outer membrane of *Pseudomonas aeruginosa*. *Mol. Microbiol. 12*, 951−958.
(27) Ramamoorthy, A., Thennarasu, S., Tan, A., Lee, D. K., Clayberger, C., and Krensky, A. M. (2006) Cell selectivity correlates with membrane-specific interactions: A case study on the antimicrobial peptide G15 derived from granulysin. *Biochim. Biophys. Acta 1758*, 154−163.
(28) Davis, J. H., Nichol, C. P., Weeks, G., and Bloom, M. (1979) Study of the Cytoplasmic and Outer Membranes of *Escherichia coli* by Deuterium Magnetic Resonance. *Biochemistry 18*, 2103−2112.
(29) Silbert, D. F., Pohlman, R., and Chapman, A. (1976) Partial Characterization of a Temperature-Sensitive Mutation Affecting Acetyl Coenzyme A Carboxylase in *Escherichia coli* K-12. *J. Bacteriol. 126*, 1351−1354.
(30) Hallock, K. J., Lee, D. K., and Ramamoorthy, A. (2003) MSI-78, an analogue of the magainin antimicrobial peptides, disrupts lipid bilayer structure via postive curvature strain. *Biophys. J. 84*, 3052−3060.
(31) Ramamoorthy, A., Thennarasu, S., Lee, D. K., Tan, A., and Maloy, L. (2006) Solid-state NMR investigation of the membrane-disrupting mechanism of antimicrobial peptides MSI-78 and MSI-594 derived from magainin 2 and melittin. *Biophys. J. 91*, 206−216.
(32) Porcelli, F., Buck-Koehntop, B. A., Thennarasu, S., Ramamoorthy, A., and Veglia, G. (2006) Structures of the dimeric and monomeric variants of magainin antimicrobial peptides (MSI-78 and MSI-594) in micelles and bilayers, determined by NMR spectroscopy. *Biochemistry 45*, 5793−5799.
(33) Yang, T. C., McDonald, M., Morrow, M. R., and Booth, V. (2009) The effect of a C-terminal peptide of surfactant protein B (SP-B) on oriented lipid bilayers, characterized by solid-state ^{2}H- and ^{31}P-NMR. *Biophys. J. 96*, 3762−3771.
(34) Roth, M. R., and Welti, R. (1994) Arrangement of phosphatidylethanolamine molecular species in *Escherichia coli* membranes and reconstituted lipids as determined by dimethyl suberimidate cross-linking of nearest neighbor lipids. *Biochim. Biophys. Acta 1190*, 91−98.
(35) Datsenko, K. A., and Wanner, B. L. (2000) One-step inactivation of chromosonal genes in *Escherichia coli* K-12 using PCR products. *Proc. Natl. Acad. Sci. U.S.A. 97*, 6640−6645.
(36) Campbell, J. W., and Cronan, J. E. Jr. (2002) The enigmatic *Escherichia coli fadE* gene is yafH. *J. Bacteriol. 184*, 3759.
(37) Davis, J. H., Jeffrey, K. R., Bloom, M., Valic, M. I., and Higgs, T. P. (1976) Quadrupolar echo deuteron magnetic resonance spectroscopy in ordered hydrocarbon chains. *Chem. Phys. Lett. 42*, 390−394.
(38) Bonev, B., and Morrow, M. R. (1996) Effects of Hydrostatic Pressure on Bilayer Phase Behaviour and Dynamics of Dilauroylphosphatidylcholine. *Biophys. J. 70*, 2727−2735.
(39) Davis, J. H. (1983) The description of membrane lipid conformation, order and dynamics by ^{2}H-NMR. *Biochim. Biophys. Acta 737*, 117−171.
(40) Silbert, D. F., Ulbright, T. M., and Honegger, J. L. (1973) Utilization of exogenous fatty acids for complex lipid biosynthesis and its effect on de novo fatty acid formation in *Escherichia coli* K-12. *Biochemistry 12*, 164−171.
(41) Russell-Schulz, B., Booth, V., and Morrow, M. R. (2009) Perturbation of DPPC/POPG bilayers by the N-terminal helix of lung surfactant protein SP-B: A ^{2}H NMR study. *Eur. Biophys. J. 38*, 613−624.
(42) Lafleur, M., Fine, B., Sternin, E., Cullis, P. R., and Bloom, M. (1989) Smoothed orientational order profile of lipid bilayers by ^{2}H-nuclear magnetic resonance. *Biophys. J. 56*, 1037−1041.
(43) Davis, J. H. (1979) Deuterium Magnetic Resonance Study of the Gel and Liquid Crystalline Phases of Diplamitoyl Phosphatidylcholine. *Biophys. J. 27*, 339−358.
(44) Morrow, M. R., Whitehead, J. P., and Lu, D. (1992) Chain-length dependence of lipid bilayer properties near the liquid crystal to gel phase transition. *Biophys. J. 63*, 18−27.
(45) Henzler-Wildman, K. A., Martinez, G. V., Brown, M. F., and Ramamoorthy, A. (2004) Perturbation of the hydrophobic core of lipid bilayers by the human antimicrobial peptide LL-37. *Biochemistry 43*, 8459−8469.
(46) Fernandez, D. I., Sani, M. A., Gehman, J. D., Hahm, K. S., and Separovic, F. (2011) Interactions of a synthetic Leu-Lys-rich antimicrobial peptide with phospholipid bilayers. *Eur. Biophys. J. 40*, 471−480.
(47) Tran, D., Tran, P. A., Tang, Y. Q., Yuan, J., Cole, T., and Selsted, M. E. (2002) Homodimeric θ-defensins from rhesus macaque leukocytes: Isolation, synthesis, antimicrobial activities, and bacterial binding properties of the cyclic peptides. *J. Biol. Chem. 277*, 3079−3084.
(48) Neidhardt, F. C., et al., Eds. (1996) *Escherichia coli and Salmonella: Cellular and molecular biology*, Vol. *1*, American Society for Microbiology, Washington, DC.
(49) Matsuzaki, K., Sugishita, K., Harada, M., Fujii, N., and Miyajima, K. (1997) Interactions of an antimicrobial peptide, magainin 2, with outer and inner membranes of Gram-negative bacteria. *Biochim. Biophys. Acta 1327*, 119−130.
(50) Matsuzaki, K., Sugishita, K., and Miyajima, K. (1999) Interactions of an antimicrobial peptide, magainin 2, with lipopolysaccharide-containing liposomes as a model for outer membranes of Gram-negative bacteria. *FEBS Lett. 449*, 221−224.
(51) Epand, R. F., Sarig, H., Mor, A., and Epand, R. M. (2009) Cell-wall interactions and the selective bacteriostatic activity of a miniature oligo-acyl-lysyl. *Biophys. J. 97*, 2250−2257.
(52) Mishra, N. N., McKinnell, J., Yeaman, M. R., Rubio, A., Nast, C. C., Chen, L., Kreiswirth, B. N., and Bayer, A. S. (2011) In vitro cross-resistance to daptomycin and host defense cationic antimicrobial peptides in clinical methicillin-resistant *Staphylococcus aureus* isolates. *Antimicrob. Agents Chemother. 55*, 4012−4018.